

I. Larin,^{1,2} D. McNulty,³ E. Clinton,⁴ P. Ambrozewicz,² P. Kingsberry,^{3,5} D. Lawrence,⁶ X. Li,⁷ I. Nakagawa,⁸
Y. Prok,³ M. Wood,⁴ A. Afanasev,⁹ A. Ahmidouch,² A. Asratyan,¹ K. Baker,⁹ L. Benton,² A. Bernstein,³
V. Burkert,⁶ P. Cole,¹⁰ P. Collins,¹¹ D. Dale,¹⁰ S. Danagoulian,² G. Davidenko,¹ R. Demirchyan,² A. Deur,⁶
A. Dolgolenko,¹ G. Dzyubenko,¹ R. Ent,⁶ A. Evdokimov,¹ J. Feng,⁷ M. Gabrielyan,⁸ L. Gan,⁷ A. Gasparian,^{2,*}
S. Gevorkyan,¹² A. Glamazdin,¹³ J. Goity,⁹ V. Goryachev,¹ V. Gyurjyan,⁶ K. Hardy,² J. He,¹⁴ M. Ito,⁶
L. Jiang,⁷ D. Kashy,⁶ M. Khandaker,⁵ A. Kolarkar,⁸ M. Konchatnyi,¹³ O. Korchin,¹³ W. Korsch,⁸
S. Kowalski,³ M. Kubantsev,¹⁵ V. Kubarovsky,⁶ V. Matveev,¹ B. Mecking,⁶ B. Milbrath,¹⁶ R. Minehart,¹⁷
R. Miskimen,⁴ V. Mochalov,¹⁸ S. Mtingwa,² S. Overby,² E. Pasyuk,¹¹ M. Payen,² R. Pedroni,² B. Ritchie,¹¹
T. Rodrigues,¹⁹ C. Salgado,⁵ A. Shahinyan,²⁰ A. Sitnikov,¹ D. Sober,²¹ S. Stepanyan,⁶ W. Stephens,¹⁷
A. Teymurazyan,⁸ J. Underwood,² A. Vasiliev,¹⁸ V. Vishnyakov,¹ B. Wojtsewski,⁶ and S. Zhou²²

¹*Alikhanov Institute for Theoretical and Experimental Physics, Moscow, Russia*

²*North Carolina A&T State University, Greensboro, NC 27411, USA*

³*Massachusetts Institute of Technology, Cambridge, MA, 02139, USA*

⁴*University of Massachusetts, Amherst, MA, USA*

⁵*Norfolk State University, Norfolk, VA 23504, USA*

⁶*Thomas Jefferson National Accelerator Facility, Newport News, VA 23606, USA*

⁷*University of North Carolina Wilmington, Wilmington, NC 28403, USA*

⁸*University of Kentucky, Lexington, NC 40506, USA*

⁹*Hampton university, Hampton, VA 23606, USA*

¹⁰*Idaho State University, Pocatello, ID, USA*

¹¹*Arizona State University, Tempe, AZ, USA*

¹²*Joint Institute for Nuclear Research, Dubna, 141980, Russia,*

On leave of absence from Yerevan Physics Institute, Yerevan, Armenia

¹³*Kharkov Institute of Physics and Technology, Kharkov, Ukraine*

¹⁴*Institute of High Energy Physics, Chinese Academy of Sciences, Beijing, China*

¹⁵*Northwestern University, Evanston/Chicago, IL, USA*

¹⁶*Pacific Northwest National Laboratory, USA*

¹⁷*University of Virginia, Charlottesville, VA, 22094, USA*

¹⁸*Institute for High Energy Physics, Protvino, Russia*

¹⁹*University of São Paulo, São Paulo, Brazil*

²⁰*Yerevan Physics Institute, Yerevan, Armenia*

²¹*The Catholic University of America, Washington, DC*

²²*Chinese Institute of Atomic Energy, Beijing, China*

(Dated: July 9, 2010)

High precision measurements of the differential cross sections for π^0 photoproduction at forward angles for two nuclei, ^{12}C and ^{208}Pb , have been performed for incident photon energies of 4.9 - 5.5 GeV to extract the $\pi^0 \rightarrow \gamma\gamma$ decay width. The experiment was done at Jefferson Lab using the Hall B photon tagger and a newly developed high resolution multichannel calorimeter. The $\pi^0 \rightarrow \gamma\gamma$ decay width was extracted by fitting the measured cross sections with recently updated theoretical models. Our result is: $\Gamma(\pi^0 \rightarrow \gamma\gamma) = 7.82 \text{ eV} \pm 1.8\% \text{ (stat.)} \pm 2.1\% \text{ (syst.)}$.

PACS numbers: 11.30.Rd, 13.40.Hq, 13.60.Le

The $\pi^0 \rightarrow \gamma\gamma$ decay is dominated by the chiral anomaly [1, 2] which is characterized by the explicit breaking of a classical symmetry by the quantum fluctuations of the quark fields when they couple to a gauge field, in general, and to the electromagnetic field of photons in this particular case. In the limit of vanishing quark masses (chiral limit) the anomaly prediction is exact, has no adjustable parameters and depends only on a few fundamental quantities: the fine structure constant, the pion decay constant, and the pion mass [1, 2]. Furthermore, in the same chiral limit the $\pi^0 \rightarrow \gamma\gamma$ decay width can be calculated exactly to all orders in perturbation theory. However, the current-quark masses are

non-vanishing and are approximately $m_u \simeq 4 \text{ MeV}$ and $m_d \simeq 7 \text{ MeV}$ for the light quarks [3, 4]. There is also a strong isospin breaking effect due to the mass difference of the up and down quarks, leading to mixing effects in the light pseudoscalar meson sector. In the past decade several new theoretical calculations of the chiral corrections have been performed based on the framework of chiral perturbation theory (ChPT) [5–7] and QCD sum rules [8]. Due to the small mass of the π^0 meson all higher order corrections are predicted to be small. As obtained in [6], the maximum enhancement of the decay width is about 4.8%, having an estimated uncertainty of less than 1%. This fact makes the $\pi^0 \rightarrow \gamma\gamma$ decay channel

a benchmark process to test the fundamental predictions of QCD in the energy range of a few GeV.

The current average experimental value for the π^0 decay width given by the PDG [3] is $\Gamma(\pi^0 \rightarrow \gamma\gamma) = 7.74 \pm 0.55$ eV. This number is an average of four experiments with much larger dispersion between both the decay width values and their quoted experimental errors, as shown in Fig. 1. The most accurate Primakoff type measurement was done at Cornell by Browman *et al.* [9] with a 5.3% quoted total error: $\Gamma(\pi^0 \rightarrow \gamma\gamma) = 7.92 \pm 0.42$ eV. Within the error bar this result agrees with the theory predictions within the error bar. Two other measurements [10, 11] with relatively large experimental errors ($\simeq 11\%$ and $\simeq 7\%$) differ significantly from each other and do not agree with the theoretical predictions. The most precise measurement of the π^0 decay width, prior to the current PrimEx experiment, was done by Atherton *et al.* [12] using the direct method of measuring the mean decay length of π^0 s produced by a high energy proton beam at CERN. Their result with the quoted 3.1% total error: $\Gamma(\pi^0 \rightarrow \gamma\gamma) = 7.25 \pm 0.18 \pm 0.14$ eV is in direct disagreement with the theoretical predictions. Clearly, a

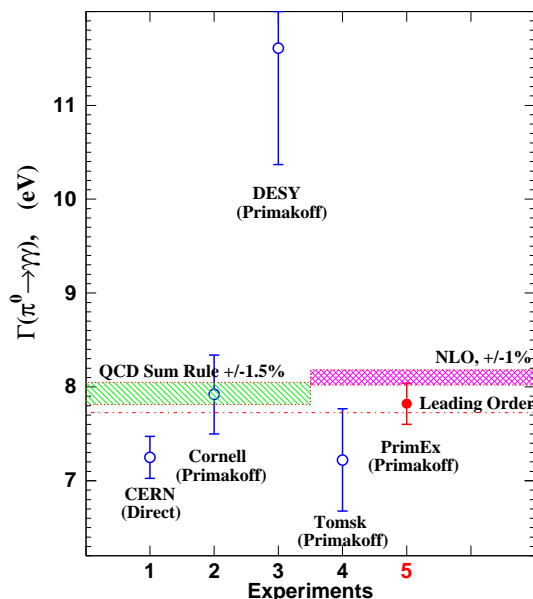


FIG. 1: $\pi^0 \rightarrow \gamma\gamma$ decay width in eV. The dashed horizontal line is the LO chiral anomaly prediction. The r.h.s. shaded band is the NLO ChPT prediction [6]. The l.h.s. shaded band is the QCD sum rule prediction [8]. The experimental results, included in the PDG average, are for: (1) the direct method [12]; (2, 3, 4) done with the Primakoff method [9–11]; (5) is the current PrimEx result.

new Primakoff type of experiment with a precision comparable to, or better than, the direct method measurement [12] was needed to address the experimental situation on this fundamental quantity. With the recent availabilities of high energy, continuous wave, high preci-

sion and high intensity photon tagging facilities, together with novel developments in electromagnetic calorimetry, it has become feasible to perform high precision cross section measurements of π^0 photoproduction on nuclei at forward directions (the Primakoff method). The combination of these two detection techniques, performed for the first time in these type of experiments, greatly improved not only the angular resolutions, which are critical for Primakoff type of measurements, but significantly reduced the systematic errors present in the previous experiments. In addition, to control and verify the precisions in the extracted values, we periodically measured the cross sections of two well known QED processes: Compton scattering and e^+e^- production with the same setup.

The present PrimEx experiment was performed in the fall of 2004 in Hall B at the Thomas Jefferson National Accelerator Facility. Incident photons with known timing and energy from the Hall B tagging facility [13] were incident on two 5% radiation length targets: ^{12}C and ^{208}Pb [14]. A large aperture collimator (12.7 mm in diameter) was used to achieve a 1% photon flux uncertainty in the experiment [15]. The relative photon tagging efficiencies were continuously measured during the experiment with the e^+e^- pair spectrometer (PS) consisting of a ~ 1.7 T·m large aperture dipole magnet and two telescopes of scintillating counters located downstream of the physical targets. The absolute normalization of the photon beam to the tagging efficiencies was measured periodically by a total absorption counter (TAC) at low beam intensities. The decay photons from $\pi^0 \rightarrow \gamma\gamma$ were detected in the multichannel Hybrid electromagnetic Calorimeter (HyCal) located at 7.5 m downstream from the physical targets to provide a large geometrical acceptance ($\sim 70\%$). The HyCal calorimeter consists of 1152 PbWO_4 crystal shower detectors ($2.05 \times 2.05 \times 18.0$ cm^3) in the central part surrounded by 576 lead glass Cherenkov counters ($3.82 \times 3.82 \times 45.0$ cm^3). Four crystal detectors are removed from the central part of the calorimeter (4.1×4.1 cm^2 hole in size) for passage of the high intensity ($\sim 10^7$ γ/s) incident photon beam through the calorimeter [16]. Twelve 5 mm thick scintillator counters, located in front of HyCal, provided rejection of charged particles and effectively reduced the background in the experiment. To minimize the decay photon conversion in air, the distance from the PS magnet to HyCal was covered by a helium bag at atmospheric pressure. The photon beam position stability during the experiment was monitored by an X-Y scintillating-fiber detector, located downstream from HyCal.

Coincidences between the photon tagger in the upper energy interval (4.9 - 5.5 GeV) and the HyCal calorimeter with a total deposited energy greater than 2.5 GeV formed the experimental trigger. The combination of the photon tagger and the calorimeter defined the following major event selection criteria in this experiment: (1) timing between the incident photon and decay photons in

the calorimeter ($\sigma_t = 1.1$ ns); (2) energy difference ΔE between the total energy in the calorimeter and the tagger ($\sigma_{\Delta E}/E = 1.8\%$); (3) invariant mass of two photons reconstructed in the calorimeter (Fig. 2).

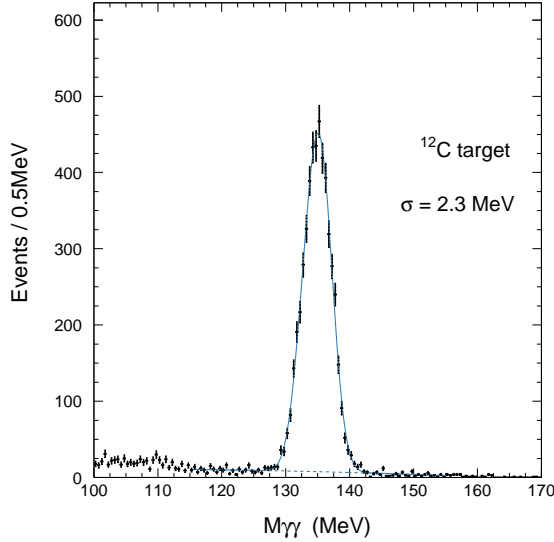


FIG. 2: Typical distribution of reconstructed invariant mass of two photons for one angular bin.

The event yield (number of π^0 events for each production angle bin) was obtained from the data by applying the selection criteria, described above, and fitting the experimental distributions for each angular bin. The typical background in the event selection process was only a few percent of the real signal events (Fig. 2). However, the uncertainty of 1.6% in the background extraction in this much upgraded experiment still remains one of the largest contributions to the total systematic error.

The extraction of differential cross sections from the experimental yields requires an accurate knowledge of the total photon flux for each tagger energy bin, the number of atoms in the target, the acceptance of the experimental setup and the inefficiencies of the detectors. The photon flux in this experiment was measured by the tagger (calibrated by the TAC) and was monitored on-line by the PS. The uncertainty reached on this important parameter was at the level of 1% [15]. Different techniques have been used to determine the number of atoms in both the targets with an uncertainty better than 0.1% [14]. The acceptance and errors on the detection efficiencies were simulated by a GEANT-based Monte Carlo code that included accurate information about the detector geometry and responses from each detector element. Other than accidental backgrounds, some physics processes with an energetic π^0 in the final state can potentially contribute to the extracted yield. It was shown that the ω photoproduction process through the $\omega \rightarrow \pi^0\gamma$ decay channel is the dominant contribution to the background. The fit

of the experimental data, as described below, with the subtracted physics background changes the extracted π^0 decay width by 1.4% with an uncertainty of 0.25%.

The resulting experimental cross sections for ^{12}C and ^{208}Pb are shown in Figs. 3 and 4 along with the fit results for individual contributions from the different π^0 production mechanisms. Two elementary amplitudes, the Primakoff (one photon exchange) T_{Pr} , and the strong (hadron exchange) T_S , contribute coherently, as well as incoherently in π^0 photoproduction off nuclei at forward angles. The cross section of this process can be expressed by four terms: Primakoff (Pr), Nuclear Coherent (NC), Interference (Int), and Nuclear Incoherent (NI):

$$\begin{aligned} \frac{d\sigma}{d\Omega} &= |T_{Pr} + e^{i\varphi}T_S|^2 + \frac{d\sigma_{NI}}{d\Omega} \\ &= \frac{d\sigma_{Pr}}{d\Omega} + \frac{d\sigma_{NC}}{d\Omega} + \frac{d\sigma_{Int}}{d\Omega} + \frac{d\sigma_{NI}}{d\Omega}, \end{aligned}$$

where φ is the relative phase between the Primakoff and the strong amplitudes. The Primakoff cross section is proportional to the π^0 decay width, the primary focus of this experiment [9]:

$$\frac{d\sigma_{Pr}}{d\Omega} = \Gamma(\pi^0 \rightarrow \gamma\gamma) \frac{8\alpha Z^2}{m^3} \frac{\beta^3 E^4}{Q^4} |F_{e.m.}(Q)|^2 \sin^2 \theta_\pi,$$

where Z is the atomic number; m , β , θ_π are the mass, velocity and production angle of the pion; E is the energy of incident photon; Q is the four-momentum transfer to the nucleus; $F_{e.m.}(Q)$ is the nuclear electromagnetic form factor, corrected for final state interactions (FSI) of the outgoing pion. The FSI effects of the photo-produced π^0 s, as well as the photon shadowing effect in nuclear matter, need to be accurately included in the cross section calculations to provide a percent level extraction of the Primakoff amplitude, and therefore, the decay width. To achieve this, and to calculate the NC and NI cross sections, a full theoretical description based on the Glauber method was developed, providing an accurate calculation of those processes in both light and heavy nuclei [17, 18]. For the NI process, an independent method based on the multi-collision intranuclear cascade model [19] was also used to double check the model dependence of the extracted decay width.

The $\Gamma(\pi^0 \rightarrow \gamma\gamma)$ decay width was extracted by fitting the experimental results with the theoretical cross sections of the four processes mentioned above folded with the angular resolutions and the measured energy spectrum of the incident photons. In the fitting process, four parameters: $\Gamma(\pi^0 \rightarrow \gamma\gamma)$, C_{NC} , C_{NI} , φ were kept free to vary the magnitude of the Primakoff, NC, NI cross sections and the phase angle, respectively. Several groups independently analyzed the experimental data. The weighted average results from these groups are presented in Table I for ^{12}C and ^{208}Pb .

Our result combined for the two targets is $\Gamma(\pi^0 \rightarrow \gamma\gamma) = 7.82 \text{ eV} \pm 1.8\% \text{ (stat.)} \pm 2.1\% \text{ (syst.)}$. The

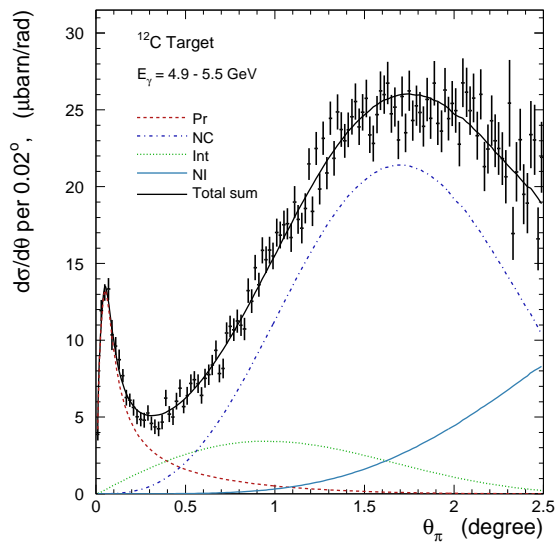


FIG. 3: Differential cross section as a function of π^0 production angle for ^{12}C together with fit results for the different physics processes (see text for explanations).

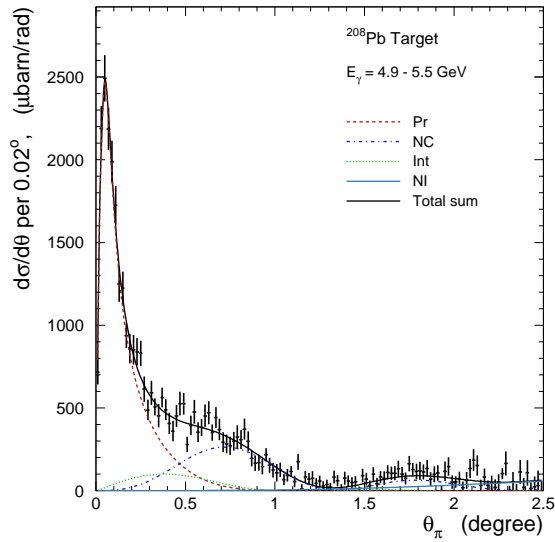


FIG. 4: Differential cross section as a function of π^0 production angle for ^{208}Pb together with fit results for the different physics processes (see text for explanations).

quoted total systematic error is the quadratic sum of all the estimated errors in this experiment including the dominant ones described above. The systematic errors in this experiment were verified by measuring the cross sections of the Compton scattering and the e^+e^- production processes. The extracted cross sections for these well known processes agree with the theory predictions at the level of 1.5% and will be published separately. Our result, with the 2.8% total experimental error, is the most precise measurement of the $\Gamma(\pi^0 \rightarrow \gamma\gamma)$ to date.

| Target | $\Gamma(\pi^0 \rightarrow \gamma\gamma)$ [eV] | C_{NC} | φ [rad] | C_{NI} | χ^2/N_{df} |
|-------------------|--------------------------------------------------|-----------------|--------------------|-----------------|-------------------|
| ^{12}C | 7.79 ± 0.18 | 0.83 ± 0.02 | 0.78 ± 0.07 | 0.72 ± 0.06 | $\frac{152}{121}$ |
| ^{208}Pb | 7.85 ± 0.23 | 0.69 ± 0.04 | 1.25 ± 0.07 | 0.68 ± 0.12 | $\frac{123}{121}$ |

TABLE I: The fit values extracted from the measured cross sections on ^{12}C and ^{208}Pb . The errors shown here are statistical only (see text for notations).

It is a factor of two-and-a-half times more precise than the current value quoted in PDG [3] on this important fundamental quantity. As a single experimental result, it directly confirms the validity of the chiral anomaly in QCD. To check the effects of chiral corrections to the anomaly, a factor of two more precise measurement is required. The second stage of this experiment is currently planned to run at Jefferson Lab within the next few years to reach the projected 1.4% precision.

We acknowledge the invaluable contributions of the Accelerator and Physics Divisions at Jefferson Lab which made this experiment possible. Special thanks go to the Hall B engineering staff for their critical contributions in all stages of this experiment. This project was supported in part by the National Science Foundation under a Major Research Instrumentation grant (PHY-0079840). The Southern Universities Research Association (SURA) operated Jefferson Lab under U.S. Department of Energy Contract No. DE-AC05-84ER40150 during this work.

* Corresponding author: gasparan@jlab.org

- [1] J.S. Bell and R. Jackiw, *Nuovo Cimento* **60A**, 47 (1969).
- [2] S.L. Adler, *Phys. Rev.* **177**, 2426 (1969).
- [3] C. Amsler *et al.*, (PDG), *Phys. Lett.* **B667**, 1 (2008).
- [4] H. Leutwyler, *Phys. Lett.* **B378**, 313 (1996).
- [5] B. Moussallam, *Phys. Rev.* **D51**, 4939 (1995).
- [6] J. Goity, A. Bernstein, B. Holstein, *Phys. Rev.* **D66**, 076014 (2002).
- [7] B. Ananthanarayan, B. Moussallam, *JHEP* **05**, 052 (2002).
- [8] B. Ioffe, A. Oganesian, *Phys. Lett.* **B647**, 389 (2007).
- [9] A. Browman *et al.*, *Phys. Rev. Lett.* **33**, 1400 (1974).
- [10] G. Bellettini *et al.*, *Nuovo Cimento* **66A**, 243 (1970).
- [11] V. Kryshkin *et al.*, *Sov. Phys. JETP*, **30**, 1037 (1970).
- [12] H.W. Atherton *et al.*, *Phys. Lett.* **B158**, 81 (1985).
- [13] D. Sober *et al.*, *Nucl. Instr. and Meth.* **A440**, 263 (2000).
- [14] P. Martel *et al.*, *Nucl. Instr. and Meth.* **A612**, 46 (2009).
- [15] <http://www.jlab.org/primex/>.
- [16] A. Gasparian, *Calorimetry in Particle Physics*, World Scientific, 109-115 (2004).
- [17] S. Gevorkyan *et al.*, *Phys. Rev.* **C80**, 055201 (2009).
- [18] S. Gevorkyan *et al.*, *hep-ph arXiv*: 0908.1297.
- [19] T.E. Rodrigues *et al.*, *Phys. Rev.* **C71**, 051603 (2005).